THE JOURNAL OF BIOLOGICAL CHEMISTRY VOL. 288, NO. 43, pp. 31080–31092, October 25, 2013

Mutations in *SLC2A2* Gene Reveal hGLUT2 Function in Pancreatic β Cell Development*

Received for publication, April 1, 2013, and in revised form, August 22, 2013 Published, JBC Papers in Press, August 28, 2013, DOI 10.1074/jbc.M113.469189

Aurélien Michau[‡1,2], Ghislaine Guillemain[§1,3], Alexandra Grosfeld[‡], Sandrine Vuillaumier-Barrot[¶], Teddy Grand[‡], Mathilde Keck[‡], Sébastien L'Hoste[‡], Danielle Chateau[‡], Patricia Serradas[‡], Jacques Teulon[‡], Pascale De Lonlay[‖], Raphaël Scharfmann[§], Edith Brot-Laroche[‡], Armelle Leturque[‡**], and Maude Le Gall[‡4]**

*From the [‡]INSERM UMRS872, Cordeliers Research Center, Université Pierre et Marie Curie, 75006 Paris, France, [§]INSERM U845, Research Center Growth and Signalling, Université Paris Descartes, Sorbonne Paris Cité, Faculté de Médecine, Hôpital Necker, 75006 Paris, France, the [¶]Biochimie et Unité Fonctionnelle de Génétique CHU Paris Nord-Val de Seine, Hôpital Xavier Bichat-Claude Bernard, 75018 Paris, France, the [‖]Reference Center of Metabolic Diseases, Necker Hospital, 75006 Paris, France, and **Institute of CardioMetabolism and Nutrition (ICAN), 75006 Paris, France*

Background: *SLC2A2* gene codes the sugar transporter-receptor hGLUT2.
Results: The study describes the impacts of gain and loss of function mutations in *SLC2A2* on pancreas development and insulin production.
Conclusion: Structure-function map of hGLUT2 is refined pointing out the importance of its sugar receptor activity.
Significance: hGLUT2 constitutes a new target to stimulate pancreatic β cell differentiation and insulin secretion.

The structure-function relationships of sugar transporter-receptor hGLUT2 coded by *SLC2A2* and their impact on insulin secretion and β cell differentiation were investigated through the detailed characterization of a panel of mutations along the protein. We studied naturally occurring *SLC2A2* variants or mutants: two single-nucleotide polymorphisms and four proposed inactivating mutations associated to Fanconi-Bickel syndrome. We also engineered mutations based on sequence alignment and conserved amino acids in selected domains. The single-nucleotide polymorphisms P68L and T110I did not impact on sugar transport as assayed in *Xenopus* oocytes. All the Fanconi-Bickel syndrome-associated mutations invalidated glucose transport by hGLUT2 either through absence of protein at the plasma membrane (G20D and S242R) or through loss of transport capacity despite membrane targeting (P417L and W444R), pointing out crucial amino acids for hGLUT2 transport function. In contrast, engineered mutants were located at the plasma membrane and able to transport sugar, albeit with modified kinetic parameters. Notably, these mutations resulted in gain of function. G20S and L368P mutations increased insulin secretion in the absence of glucose. In addition, these mutants increased insulin-positive cell differentiation when expressed in cultured rat embryonic pancreas. F295Y mutation induced β cell differentiation even in the absence of glucose, suggesting that mutated GLUT2, as a sugar receptor, triggers a signaling pathway independently of glucose transport and metabolism. Our results describe the first gain of function mutations for hGLUT2, revealing the importance of its receptor *versus* transporter function in pancreatic β cell development and insulin secretion.

The *SLC2A2* gene product GLUT2 is a low affinity facilitative glucose transporter expressed in tissues involved in glucose homeostasis, *i.e.*, liver, pancreatic β cells, kidney, and intestine (1). In addition to allowing transmembrane transport of sugar, GLUT2 is proposed to be a glucose detector. Together with glucokinase, a high K_m hexokinase, GLUT2 is fueling intracellular metabolism and triggers adequate insulin secretion by pancreatic be β cells (2). A GLUT2 specific extracellular glucose sensing pathway exists in cultured β pancreatic, hepatoma, and enterocytic cells (3–6). This pathway targeting glucose-sensitive gene expression engages nuclear importers (4, 5, 7). In addition to its transporter function, GLUT2 has therefore the property to trigger a signaling cascade in response to changes of extracellular glucose concentrations whatever the level of intracellular energy stores (8, 9). The relative impacts of these two independent but complementary GLUT2 functions, sugar transporter *versus* extracellular sugar receptor, have been poorly explored.

Some genetic defects within *SLC2A2* gene cause Fanconi-Bickel syndrome (FBS)[5] (10). FBS is due to homozygous or compound heterozygous mutations in *SLC2A2*, suggesting that a single unaltered allele is sufficient to fulfill vital protein functions. This is consistent with an autosomal recessive pattern of inheritance. So far, over 100 cases are reported in the world, and mutation analyses have revealed a total of 34 different *SLC2A2* point mutations with no particular hot spot (10).

* The work was supported by Institut National de la Santé et de la Recherche Médicale (INSERM), Université Pierre & Marie Curie Paris 6 (UMPC) and Université René Descartes Paris 5, Centre National de la Recherche Scientifique (CNRS), and the 6th European Union Framework Program (Beta-Cell Therapy Integrated Project) (to R. S.).
[1] Both authors contributed equally to this work.
[2] Recipient of a doctoral fellowship from UPMC Paris 6.
[3] Present address: INSERM UMRS872; Cordeliers Research Center; Université Pierre et Marie Curie; Paris, France.
[4] To whom correspondence should be addressed. INSERM U773, Université Paris Diderot Paris 7, Faculté de Médecine Site Bichat, 16 Rue Henri Huchard, 75890 Paris Cedex 18, France. Tel.: 33-157-277-459; Fax: 33-157-277-471; E-mail: maude.le-gall@inserm.fr.

[5] The abbreviations used are: FBS, Fanconi-Bickel syndrome; 2-DOG, 2-deoxy-D-glucose; SNP, single-nucleotide polymorphism; TM, transmembrane domain.

More than 70% of mutations result in truncated proteins (frameshift, nonsense, splice site mutations), suggesting that an inactive protein is responsible for the disease. In addition, 10 missense mutations are described in FBS. These mutations are only described at the genomic level. FBS patients suffer from hepatomegaly, nephromegaly, glucose-galactose malabsorption, gross urinary loss of glucose, and failure to thrive (10). Furthermore, an adult FBS patient is reported to have developed gestational diabetes during pregnancy (11). In some cases, patients show low insulinemia and diabetes (12, 13). The diabetes can occur transiently during the neonatal period (14). These subjects have low birth weight, indicative of a possible lack of insulin *in utero*. Whether GLUT2 plays an active role in human pancreas has long been discussed (15). GLUT2 is probably not a major transporter fueling glucose flux and metabolism in adult human pancreatic β cells, and its implication in type 2 diabetes is still controversial (16–20). Nevertheless, in neonates and children, GLUT2 is more abundant (21). A role of GLUT2 is thus more likely to occur during the developmental and neonatal periods in humans.

There is no crystal structure for members of the GLUT family yet. However, the crystal structures of other members of the sugar porter family, bacteria lactose permease (LacY) (22), fucose permease (FucP) (23), and xylose symporter (XylE) (24), are solved. Two states, inward open and outward open conformations, are representative of permeases exposed to extracellular or intracellular sugar, respectively. These structures are used to propose *in silico* models of mammalian GLUT members (24–26). Furthermore, cysteine scanning mutagenesis (27), biochemical analyses (25), and *in silico* analysis (26) allow the modeling of GLUT1 sugar channel as an hydrophilic cavity created by a specific organization of transmembrane helices. Nevertheless, the functioning of GLUT1 is still not fully understood. Invariant or highly conserved amino acids among the families of prokaryotic or eukaryotic sugar porters pinpoint amino acids that might be important for structure or functions. *In vitro* or *in vivo* characterization of mutated proteins is required to identify key amino acids associated with protein functions. A functional study was conducted for the V197I mutation in *SLC2A2*, discovered as a single allele mutation in a type 2 diabetic subject; it abolishes GLUT2 transport activity (28). Activating mutations of GLUT2 have not been reported yet; they might create symptoms opposite to those of FBS patients such as exacerbated insulin secretion.

In this study, we fully characterized nine mutations scattered through the *SLC2A2* gene to identify potential amino acid differentially involved in the two hGLUT2 functions: transporter and receptor. To this aim, we performed detailed analyses of membrane expression profiles in hepatic and pancreatic β cells, transport kinetics in *Xenopus* oocytes, glucose-induced insulin secretion, and development of pancreatic β cells.

EXPERIMENTAL PROCEDURES

Sequence Alignment and Topology of Human GLUT2—Topology of human GLUT2 was realized with the Topo2 program with predicted transmembrane sequences found in UniProtKB/Swiss-Prot. Multiple sequence alignment of GLUT2 homologs and orthologs were realized with BLASTP. Protein sequences were found in the UniProtKB database: P11166 for human GLUT1; P14672 for human GLUT4; P11168 for human GLUT2; H2QNR0 (predicted) for chimpanzee (*Pan troglodytes*); P14246 for mouse (*Mus musculus*) GLUT2; P12336 for rat (*Rattus norvegicus*) GLUT2; Q90592 for chicken (*Gallus gallus*) GLUT2; Q102R8 for zebrafish (*Danio rerio*) GLUT2; P32465 for yeast (*Saccharomyces cerevisiae*) HXT1; and Q9FRL3 for plant (*Arabidopsis thaliana*) sugar transporter protein STP1.

Molecular Biology—Human *SLC2A2* gene (GenBank™ accession number NM_000340.1) was obtained from RZPD (IMAGp958A041562Q) and HA-tagged after subcloning into pIRES-3HA-hrGFP vector (Stratagene). *SLC2A2* mutants were obtained by site-directed mutagenesis. All constructs were fully sequenced. pIres-hGLUT2–3HA-hrGFP constructs were subcloned in a pSDeasyBS vector to be used for *in vitro* transcription and expression in *Xenopus* oocytes. Some constructs were also subcloned into adenoviral expression vectors (GeneCust) for infection of cells and rat pancreases. The extracellular C-terminal HA tag that facilitates detection had no discernible effect on either expression or function of the wild-type transporter.

Expression in Xenopus Oocytes—Capped cRNA were synthesized *in vitro* from hGLUT2 expression vectors linearized with FspI using the mMessage mMachine SP6 kit (Ambion). *Xenopus* oocytes (EcoCyte Bioscience), kept at 18 °C in modified Barth's solution containing 88 mM NaCl, 1 mM KCl, 0.41 mM $CaCl_2$, 0.32 mM $Ca(NO_3)_2$, 0.82 mM $MgSO_4$, 10 mM HEPES, pH 7.4, and gentamycin (20 mg/ml), were injected with 75 ng of the different cRNA and incubated for 48 h before experiments. Surface labeling of *Xenopus* oocytes was performed as described (29) using hGLUT2 antibody (MAB 1414; R&D Systems).

Uptake of Radiolabeled 2-Deoxy-D-glucose—Five injected *Xenopus* oocytes were incubated in 500 μl of modified Barth's solution containing 2.5–100 mM 2-deoxy-D-glucose (2-DOG) and 0.5 μCi of [^{14}C]2-DOG as tracer (PerkinElmer Life Sciences) for 10 min at 20 °C in initial rate conditions. Uptake was stopped by washes with ice-cold buffer containing 2 mM $HgCl_2$. A single oocyte was lysed with 500 μl of SDS 10% before radioactivity counting (1600TR; Packard). At least three independent experiments were performed for each construct. Uptakes were expressed as nmol/min/oocyte, and K_m and V_{max} kinetic parameters were calculated with Kaleidagraph software, using the Michaelis-Menten equation. *Xenopus* oocytes are devoid of endogenous *SLC2A* ortholog genes.

Cell Culture, Transfection, and Infection—The mhAT3F hepatoma cell line and MIN6 pancreatic β cell line were grown as described previously (30, 31). The MIN6 cell line is one of the few β cell lines that can secrete insulin in response to glucose. However, MIN6 cells have a large expression of wild-type mouse GLUT2 that could minimize the consequences of hGLUT2 expression. Hepatoma mhAT3F and pancreatic MIN6 cells were transfected with Lipofectin or Lipofectamine 2000 according to the manufacturer's instructions (Invitrogen). Infections of mhAT3F or MIN6 cells were performed as recommended by the manufacturer (GeneCust) with 5000 viral particles/cell in the absence of serum. After 2 h, the viruses were washed out, and the cells were supplied with complete growth

medium. Analyses were performed 48 h after transfection or infection.

Immunofluorescence Analyses—Immunofluorescence on mhAT3F or MIN6 cells were performed as previously described (3, 5) with anti-HA (sc-805; Santa Cruz), anti-hGLUT2 (directed against extracellular epitope of hGLUT2, MAB1414; R&D Systems), and anti-E-cadherin (TAK-M108, Takara) followed by cyanin-coupled secondary antibodies (715-165-150, 711-165-152, and 712-225-153; Jackson ImmunoResearch Laboratories Inc.).

Protein Expression—Total membrane proteins were prepared using the ProteoJet membrane protein extraction kit (Fermentas) according to the manufacturer's instructions and analyzed by Western blot with anti-HA (sc-805; Santa Cruz), anti-E-cadherin (TAK-M108; Takara), and peroxidase-coupled secondary antibodies (Amersham Biosciences). Detection was performed with ECL (Amersham Biosciences) and ImageQuant LAS 4000 (GE Healthcare) subsequently quantified by densitometry using the Multi-Gauge V2.3 program (Fuji Photo Film Co.).

FACS Analysis—mhAT3F or MIN6 cells were detached with trypsin and suspended in binding buffer (D-PBS 0.15% BSA). Cell suspensions were incubated for 1 h with anti-hGLUT2 conjugated to phycoerythrin antibody (directed against extracellular epitope of hGLUT2, FAB1414P; R&D Systems), diluted in binding buffer. Cells were washed three times with fresh D-PBS, and the fluorescence of each sample was evaluated using BD LSRII FACS system and BD FACS Diva software (Becton Dickinson). The results were analyzed using the FlowJo software (Tree Star, Inc).

RNA Levels—Total RNA from mhAT3F or MIN6 cells was extracted using TriReagent (MRC). Reverse transcription was carried out with 1 μg of total RNA according to the manufacturer's protocol (Roche Applied Science), and messenger DNA was quantified with a Mx3000 real time PCR system (Stratagene). ProbeFinder version 2.45 (Roche Applied Science) was used to design specific primers for m-Insulin. m-LPK, m-GLUT2, and m-Cyclophillin primers were previously described (32).

Pancreatic Explant Infection and Culture—All animal manipulations were realized in compliance with the French Animal Care Committee's guidelines. Dorsal pancreatic explants from embryonic day 13.5 Wistar rat embryos were dissected, dissociated, infected, and cultured as previously described (33). Briefly, at the end of the dissociation, cells were dispatched in 1.5-ml tubes (5×10^4 cells/tube) in complete RPMI culture medium (Lonza) supplemented with 10% heat-inactivated FCS (HyClone) and ROCK inhibitor (7 μg/ml; Sigma-Aldrich), in the presence or absence of glucose. During an overnight period, cells reaggregated and formed clusters that were transferred on 0.45-μm filters (Millipore) and cultured for 6 additional days in complete RPMI culture medium. For adenoviral infection, dissociated cells were cultured for 2.5 h at 37 °C in 50 μl of RPMI 1640 with adenoviruses (multiplicity of infection of 2) producing hGLUT2 variants or a dominant-negative form of ChREBP previously described (34). At the end of the infection period, complete RPMI medium was added, and cells were reaggregated as described above before being transferred on filters for six additional days. Infected pancreases were treated the same way as noninfected ones.

Pancreatic Explant Staining and Quantification—Tissues were fixed in 10% formalin and embedded in paraffin. All sections (4 μm thick) of pancreatic explants were collected and processed for immunohistochemical analysis with mouse anti-insulin, rabbit anti-insulin, rabbit anti-amylase, rabbit anti-glucagon (Sigma-Aldrich), and mouse anti-BrdU (Amersham Biosciences). The fluorescent secondary antibodies used included fluorescein anti-rabbit and Texas Red anti-mouse (Jackson ImmunoResearch Laboratories Inc.) and Alexa Fluor 488 anti-rabbit (Invitrogen). The nuclei were stained with Hoechst 33342 (Invitrogen). All sections from each pancreatic explants were digitized with a camera (Hamamatsu) linked to a fluorescence microscope (Leitz DMRB; Leica). Each image was quantified using ImageJ 1.34 s, and sums give the total surface/explant in mm^2. At least four explants were analyzed per condition.

To quantify the proliferation of insulin- and amylase-positive cells, the frequency of BrdU-positive nuclei among 2,000 insulin- or amylase-positive cells/bud were counted. At least three explants grown under each set of culture conditions were analyzed.

Electron Microscopy—Infected or noninfected pancreatic explants were fixed at 4 °C for 2 h in 2.5% glutaraldehyde, in 0.1 M phosphate buffer, pH 7.3, postfixed for 1 h in 1%, buffered osmium tetroxide, dehydrated, and embedded in Epon 812. Thin sections were placed on uncoated 200-mesh nickel grids. For immunoelectron microscopy, sections were etched with 0.5 M of sodium metaperiodate for 1 h at room temperature and incubated overnight at 4 °C with anti-insulin (Dako A564) and then with 18-nm gold reagent for 1 h and with IgG coating colloidal gold particles (Jackson ImmunoResearch Laboratories Inc.). The sections were counterstained with 2% aqueous uranyl acetate for 30 min and then with lead citrate for l0 min and viewed under a Philips 100× electron microscope.

Glucose-induced Insulin Secretion—Glucose-induced insulin secretion assays were performed in MIN6 cells or pancreases infected with adenoviral vectors. For infected MIN6 cells, 48 h after infection, the cells were preincubated for 30 min at 37 °C in Krebs-Ringer bicarbonate buffer (10 mM HEPES, 120 mM NaCl, 4.7 mM KCl, 1.2 mM $MgSO_4$, 1.2 mM KH_2PO_4, 20 mM $NaHCO_3$, 2 mM $CaCl_2$, 0.5% BSA, pH 7). Cells were then incubated with Krebs-Ringer bicarbonate buffer supplemented or not with 1, 5, or 25 mM glucose for 2 h.

For infected pancreases cultured for 7 days in presence of 10 mM glucose, glucose was removed for 1 h before the glucose-induced insulin secretion assay. Pancreases were then incubated with fresh medium supplemented or not with 10 mM glucose for 2 h.

Culture media were collected after 30, 60, and 120 min, centrifuged (12,000 rpm; 2 min; 4 °C), and supernatants were stored at −20 °C until insulin quantification. Insulin concentrations were measured with ELISA kit rat/mouse insulin (EZRMI-13K; Millipore).

Statistics—The results are presented as the means ± S.E. of three to five experiments or assays. Statistical analysis was performed using STATEL software (AdScience), and significance

($p < 0.05$) was established using Kruskal-Wallis and Mann-Whitney tests.

RESULTS

hGLUT2 Variants—To build a structure-function map of hGLUT2, we analyzed nine *SLC2A2* variants (Table 1). Mutants c.59G>A p.Gly20Asp, c.726C>A p.Ser242Arg c.1250C>T p.Pro417Leu, and c.1330T>C p.Trp444Arg were chosen among 10 missense mutations in families carrying mutations associated with FBS, expected to display null phenotype (*i.e.*, no hGLUT2 function) (10). As represented on Fig. 1, G20D mutation is located in the first transmembrane domain, S242R mutation is positioned in a sugar transporter signature PESPR, P417L mutation affects an invariant amino acid in transmembrane domain 10, and W444R mutation is situated in a putative sugar-binding site of the sugar channel.

In parallel, three mutations in invariant or highly conserved amino acids were generated: c.58G>A p.Gly20Ser, c.884T>A p.Phe295Tyr, and c.1103T>C p.Leu368Pro. G20S is a mutation at a similar position giving FBS when mutated in Asp, F295Y disturbs a highly conserved amino acid in the large intracytoplasmic domain triggering sugar signaling, and L368P affects highly conserved amino acid in the sugar porter family (Fig. 1). Furthermore, two *SLC2A2* SNP (c.329C>T p.Thr110Ile (T110I; SNP rs5400 G/A) and c.203C>T p.Pro68Leu (P68L; SNP rs7637863 G/A)) variants were studied as controls.

TABLE 1
***SLC2A2* mutations**

Nucleotide change[a]	Predicted amino acid change[b]
Nonsynonymous SNPs	
c.203C>T	p.Pro68Leu (P68L)
c.329C>T	p.Thr110lle (T110I)
FBS-associated mutations[c]	
c.59G>A	p.Gly20Asp (G20D)
c.726C>A	p.Ser242Arg (S242R)
c.1250C>T	p.Pro417Leu (P417L)
c. 1330T>C	p.Trp444Arg (W444R)
Additional missense mutations	
c.58G>A	p.Gly20Ser (G20S)
c.884T>A	p.Phe295Tyr (F295Y)
c.1103T>C	p.Leu368Pro (L368P)

[a] Reference sequence: NM_000340.1.
[b] Reference sequence: NP_000331.1.
[c] These FBS-associated mutants were reviewed in Ref. 10.

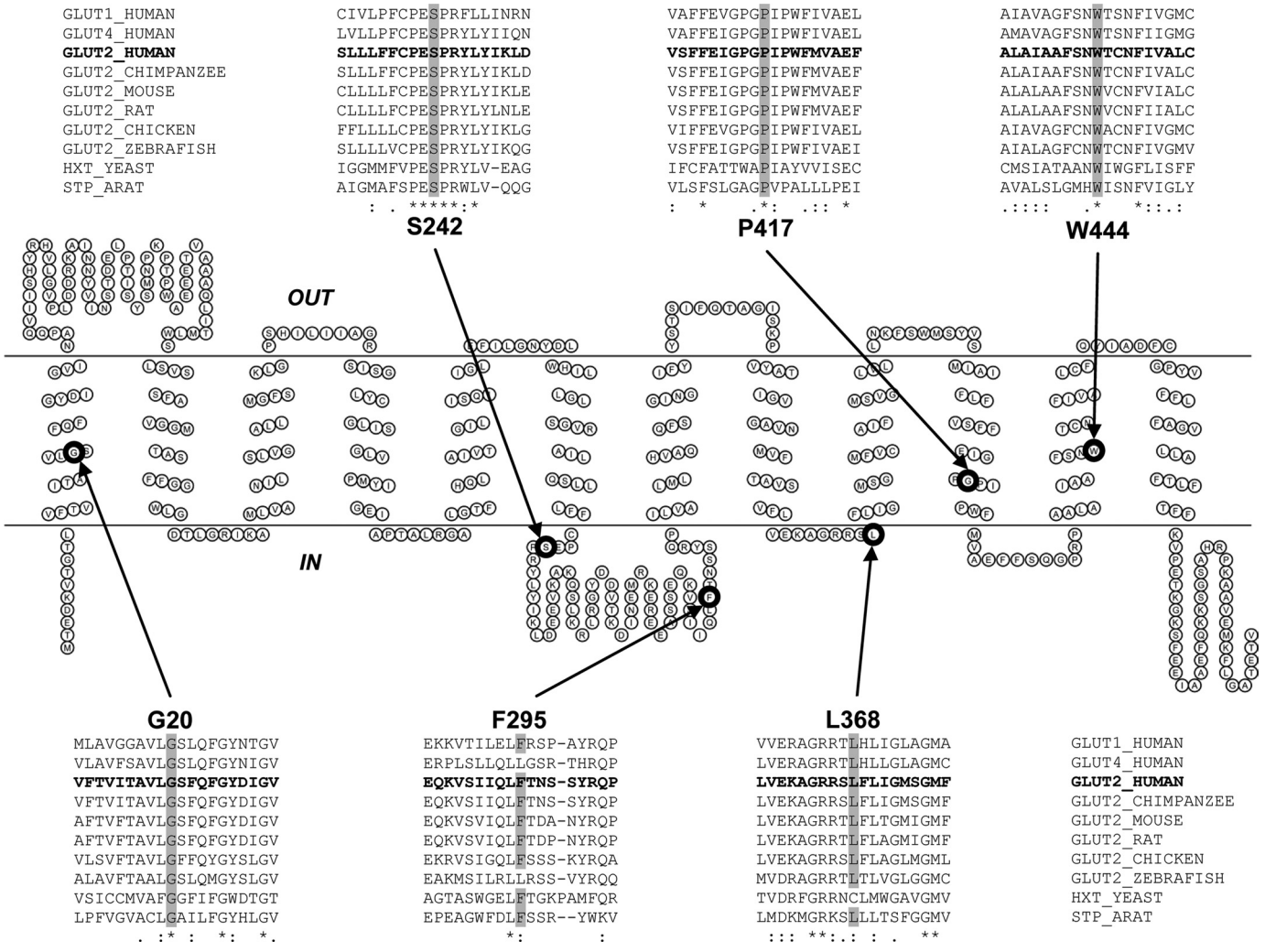

FIGURE 1. **Topology and amino acid alignments of human GLUT2.** The figure shows the topology of human GLUT2 with the location of conserved amino acids (in *gray* Gly-20, Ser-242, Phe-295, Leu-368, Pro-417, and Trp-444) analyzed in this study. Evolutionary conservation is shown by multiple sequence alignment with BLASTP of GLUT2 homologs: human GLUT1 and GLUT4, chimpanzee GLUT2, mouse GLUT2, rat GLUT2, chicken GLUT2, zebrafish GLUT2, yeast *S. cerevisiae* HXT1, and plant *A. thaliana* STP1.

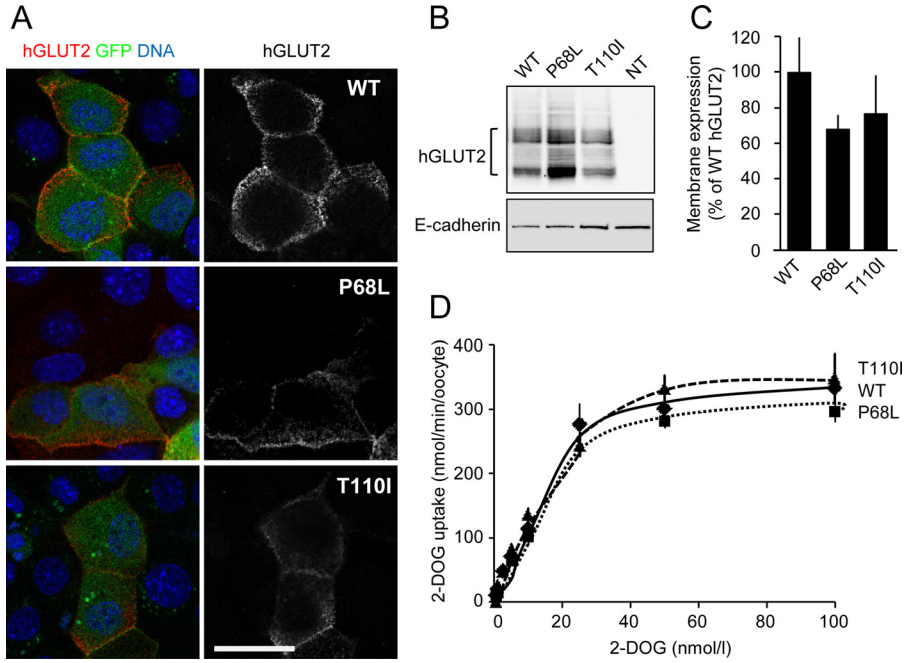

FIGURE 2. **Expression and transport function of two SNP variants of hGLUT2.** *A*, expression of hGLUT2 wild type (*WT*) and two SNP variants (P68L and T110I) in mhAT3F cells. Cells transfected with a pCMV-hGLUT2-HA-IRES-hrGFP construct are identified by the expression of the GFP. Plasma membrane location of hGLUT2 (*red* in the *left panels* and *white* in the *right panels*) is revealed with an antibody to an extracellular epitope of hGLUT2 in nonpermeabilized cells. Nuclei are stained with DAPI (*blue*). *Scale bar* corresponds to 25 μm. *B*, Western blot analysis of membrane fractions from mhAT3F cells transfected or not transfected (*NT*) with different hGLUT2 constructs. hGLUT2 expression is revealed with an antibody to HA epitope. E-cadherin is used as a loading control of membrane fractions. *C*, membrane expression of WT, P68L, and T110I hGLUT2 in *Xenopus* oocytes injected with the corresponding cRNAs. *D*, dose-response curves of 2-DOG uptake by *Xenopus* oocytes injected with WT, P68L, or T110I hGLUT2 cRNA. *Curves* are fitted up using Michaelis-Menten nonlinear regression.

Subcellular Location and Transport Function of SNP Variants of hGLUT2—Expression and location of hGLUT2 wild type and variants were characterized by immunofluorescence analyses using an antibody recognizing extracellular epitopes on nonpermeabilized mhAT3F hepatoma cells (Fig. 2*A*). Furthermore, their membrane location was confirmed by co-localization with the membrane-resident protein E-cadherin in the membrane fractions analyzed by Western blot (Fig. 2*B*). The immunofluorescence and Western blot analyses of the P68L and T110I hGLUT2 polymorphisms indicated that their expression, location, and size were similar to that of wild-type hGLUT2 (Fig. 2, *A* and *B*).

Uptake of 2-DOG was measured in *Xenopus* oocytes expressing similar membrane levels of WT, P68L, and T110I hGLUT2 (Fig. 2, *C* and *D*). The saturation curves were performed, and K_m and V_{max} parameters were calculated (Table 2). They were similar to kinetic parameters previously published by others for hGLUT2 (35). The isoleucine 110 substitution (T110I) as previously described (28) and the leucine 68 substitution (P68L) in this study did not appreciably affect transport characteristics (Fig. 2*D* and Table 2).

FBS hGLUT2 Mutants—Many FBS case reports published previously assumed that homozygous or compound heterozygous mutations identified in *SLC2A2* would be responsible for a functionally dead GLUT2 transporter. Whereas this assumption seems reasonable for mutation resulting in truncated proteins, it remains to be comprehensively tested for single-nucleotide missense mutations. In the present investigation, we therefore functionally characterized four missense mutations associated to FBS (G20D, S242R, P417L, and W444R) (Fig. 3).

TABLE 2
Kinetic parameters of hGLUT2 mutants using 2-DOG

hGLUT2	K_m	V_m
	mM of 2-DOG	*nmol/min/oocyte*
WT	22 ± 3	422 ± 20
SNP		
P68L	24 ± 4	384 ± 20
T110I	20 ± 4	436 ± 30
Additional missense mutations		
G20S	30 ± 6[a]	540 ± 45[a]
F295Y	17 ± 3[b]	300 ± 18
L368P	23 ± 4	215 ± 15[a]

[a] $p < 0.001$.
[b] $p < 0.01$ in comparsion with WT.

FBS-associated G20D mutant was undetectable in both immunofluorescence and Western blot assays (Fig. 3, *A* and *B*), indicating that it was either not translated or rapidly degraded by the cell protein control process. S242R mutant was barely detected and not targeted at the plasma membrane (Fig. 3, *A* and *B*), suggesting defects in the translation, maturation, and/or targeting processes of the corresponding mutated hGLUT2 protein. In contrast, P417L and W444R mutants were expressed in cell plasma membrane and displayed the expected hGLUT2 size, confirming the membrane location of full size proteins (Fig. 3, *A* and *B*). This was observed in mhAT3F cells (Fig. 3, *A* and *B*), as well as in MIN6 cells (not shown) or in *Xenopus* oocytes (Fig. 3*C*). In all transfection assays, GFP was identified assessing a proper expression of the plasmid constructs (Figs. 2*A* and 3*A*, *left panels*). *Xenopus* oocytes were injected with cRNA coding FBS mutants that could be detected in mammalian cells (S242R, P417L, and W444R) to assay their transport capacities. S242R mutant exhibited no protein at the

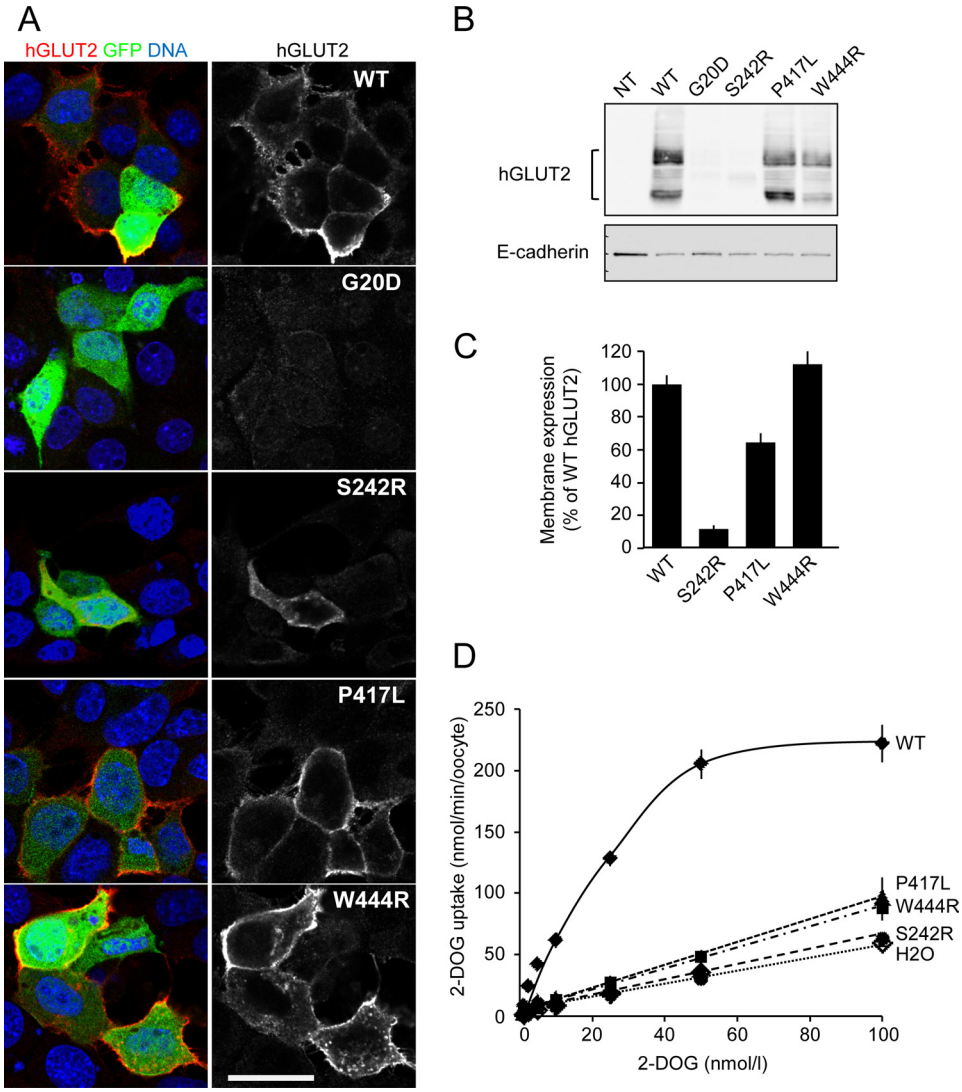

FIGURE 3. **Expression and transport function of four FBS-associated mutants of hGLUT2.** *A*, expression of hGLUT2 wild type (*WT*) and four FBS-associated mutants (G20D, S242R, P417L, and W444R) in mhAT3F cells. Cells transfected with a pCMV-hGLUT2-HA-IRES-hrGFP construct are identified by the expression of the GFP. Subcellular location of hGLUT2 (*red* in the *left panels* and *white* in the *right panels*) is revealed with an antibody to HA epitope in permeabilized cells. Nuclei are stained with DAPI (*blue*). Note that G20D hGLUT2 cannot be detected, and S242R hGLUT2 is not targeted at the plasma membrane. *Scale bar* corresponds to 25 μm. *B*, Western blot analysis of membrane fractions from mhAT3F cell transfected or not transfected (*NT*) with different hGLUT2 constructs. hGLUT2 expression is revealed with an antibody to HA epitope. E-cadherin is used as a loading control of membrane fractions. Note that G20D or S242R hGLUT2 cannot be detected in membrane fractions. *C*, membrane expression of WT, S242R, P417L, and W444R hGLUT2 in *Xenopus* oocytes injected with the corresponding cRNAs. *D*, noncorrected uptake of 2-DOG by *Xenopus* oocytes injected with water or injected with WT, S242R, P417L, or W444R hGLUT2 cRNA.

plasma membrane of *Xenopus* oocyte (Fig. 3*C*), and the resulting uptake of 2-DOG was identical to that of oocytes injected with water (Fig. 3*D*). Oocytes expressing similar membrane levels of the FBS P417L and W444R hGLUT2 mutants (Fig. 3*C*) displayed no specific 2-DOG uptake (Fig. 3*D*). Our results demonstrate that the four FBS-associated *SLC2A2* mutants lack hGLUT2 transport function contributing to the FBS phenotype and support the important role of hGLUT2 transporter fueling metabolism at body level.

Missense hGLUT2 Mutants—In addition to FBS mutants, we characterized three additional mutants designed to affect invariant or highly conserved amino acids of the sugar porter family (G20S, F295Y, and L368P; Fig. 1). We expressed these mutants in mhAT3F and MIN6 cell lines. They were properly targeted at cell plasma membranes as assayed by immunofluorescence showing their co-localization with the membrane-resident protein E-cadherin (Fig. 4*A*) or by FACS analysis on non-permeabilized cells (Fig. 5*A*). They also revealed similar patterns in Western blot analysis of membrane extracts when compared with wild-type hGLUT2 (Fig. 4*B*).

2-DOG uptake was measured in *Xenopus* oocytes expressing similarly wild-type or mutant hGLUT2 (Fig. 4, *C* and *D*) to calculate K_m and V_{max} parameters (Table 2). F295Y hGLUT2 showed 25% increase in sugar affinity ($1/K_m$) ($p < 0.01$) but 30% decrease in V_{max} (transport capacity) ($p < 0.001$) as compared with wild-type hGLUT2. Thus, this mutation may not modify significantly sugar fluxes at physiological glucose concentrations. G20S mutant showed 35% lower sugar affinity ($p < 0.001$), a similar sugar flux up to 30 mM, but a V_{max} 28% higher ($p < 0.001$) than wild-type hGLUT2. By contrast, L368P mutant showed an affinity similar to wild-type hGLUT2, but its V_{max} was decreased by 50% ($p < 0.001$). These modifications of

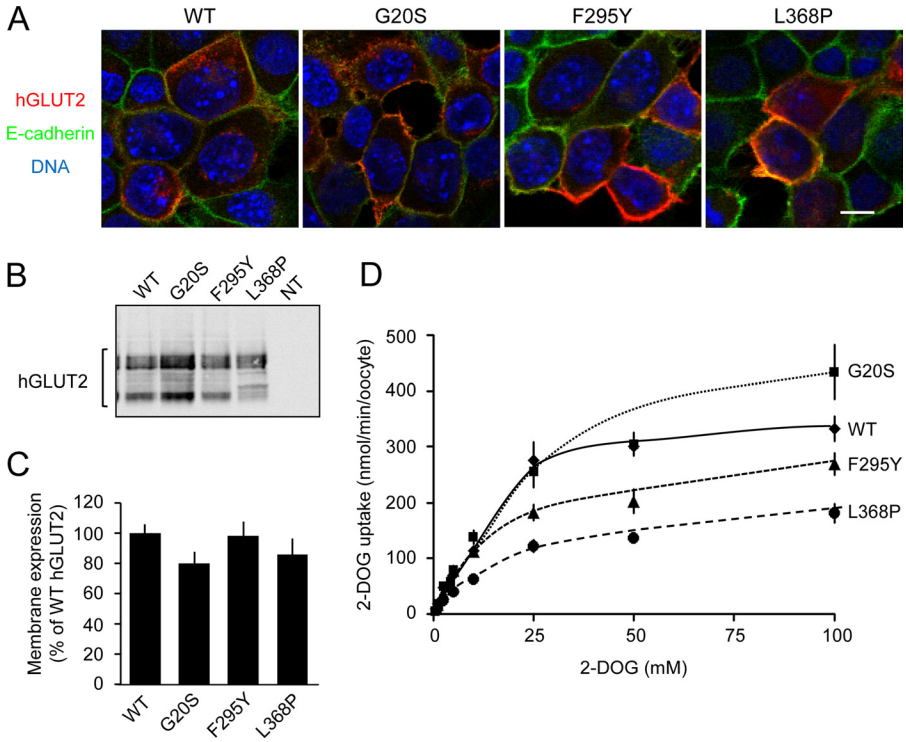

FIGURE 4. **Expression and transport functions of three engineered mutants of hGLUT2.** *A*, membrane co-localization of wild type (*WT*), G20S, F295Y, and L368P hGLUT2 (*red*) and membrane marker E-cadherin (*green*) in infected mhAT3F cells analyzed by confocal microscopy. Nuclei are stained with DAPI (*blue*). *Scale bar* corresponds to 10 μm. *B*, similar migrating profiles of hGLUT2 WT and mutants (G20S, F295Y, and L368P) in membrane fractions of mhAT3F cells analyzed by Western blot. *C*, comparable membrane expression of WT, G20S, F295Y, and L368P hGLUT2 in *Xenopus* oocytes injected with the corresponding cRNAs. *D*, dose-response curves of 2-DOG uptake by *Xenopus* oocytes injected with WT, G20S, F295Y, and L368P hGLUT2. *Curves* are fitted up using Michaelis-Menten nonlinear regression.

glucose transport kinetic parameters by hGLUT2 mutants prompted us to test their impact on insulin secretion and pancreatic cell development.

Glucose-induced insulin secretion in pancreatic cell lines requires the expression of GLUT2 (15, 36). We thus measured insulin secretion in MIN6 cells that express large amounts of endogenous (murine) GLUT2 (31), assuming that heterotetramer formation between endogenous murine and mutant human GLUT2 might reveal altered function. The proportion of MIN6 pancreatic cells expressing hGLUT2 after infection was similar for each mutant (Fig. 5*A*) and allowed comparison of the functional impact of the three missense mutations. Neither insulin mRNA nor protein content were significantly affected by expression of hGLUT2 mutants (Fig. 5, *B* and *C*). As expected, insulin secretion per cell increased in response to glucose in a dose-dependent manner (1 mM *versus* 5 mM *versus* 25 mM) in MIN6 cells expressing wild-type or mutant hGLUT2 (Fig. 5*D*). Glucose-induced insulin secretion profile was not grossly modified by F295Y hGLUT2 expression. On the contrary, G20S hGLUT2 expression amplified glucose-induced insulin secretion at 1, 5, and 25 mM glucose as compared with wild-type hGLUT2, suggesting that this mutant exerts a dominant function over endogenous murine GLUT2. This could be due either to accelerated transport (Fig. 4*D* and Table 2) or increased signaling activity. Interestingly, in the total absence of glucose, basal insulin secretions by MIN6 cells expressing G20S or L368P hGLUT2 were significantly higher as compared with cells expressing wild-type hGLUT2 (Fig. 5*E*). Thus, G20S and L368P appeared as potential gain of function hGLUT2 mutations promoting insulin secretion by β cells in the absence of glucose. At higher glucose concentration (25 mM), the potential gain of function L368P hGLUT2 receptor is counterbalanced by its reduced V_{max} transporter (Fig. 4*D* and Table 2), resulting in insulin secretion similar to that of wild-type hGLUT2 (Fig. 5*D*).

The impact of hGLUT2 engineered mutations on pancreatic β cell differentiation was addressed (Fig. 6). The development of rat embryonic pancreases, expressing hGLUT2 wild type or mutants, was analyzed after 7 days of culture in the presence or absence of added glucose (10 mM). As expected, in control non-infected pancreases, the positive effect of glucose on β cell differentiation was observed, because the insulin-positive cell surface increased 3-fold (Fig. 6*A*, with quantification in Fig. 6*B*) (37). Expression of wild-type hGLUT2 did not favor pancreatic β cell development (Fig. 6*A*, with quantification in Fig. 6*B*). The infection of pancreatic explants with G20S and L368P hGLUT2 further increased the surface of insulin-positive cells in the presence of glucose when compared with infection with wild-type hGLUT2 (Fig. 6*A*, with quantification in Fig. 6*B*). F295Y hGLUT2 expression drastically increased, in the absence of glucose, the insulin-positive cell surface that did not further increase after glucose addition (Fig. 6*A*, with quantification in Fig. 6*B*). F295Y mutant thus mimicked the effect of glucose addition, activating constitutively the sugar-signaling pathway that triggers β cell differentiation. The developments of α cells (*i.e.*, glucagon-positive cells) or exocrine cells (*i.e.*, amylase-positive cells) were not affected (Fig. 6, *C* and *D*). Finally, the proliferation indices, as assayed by BrdU incorporation, in insulin-

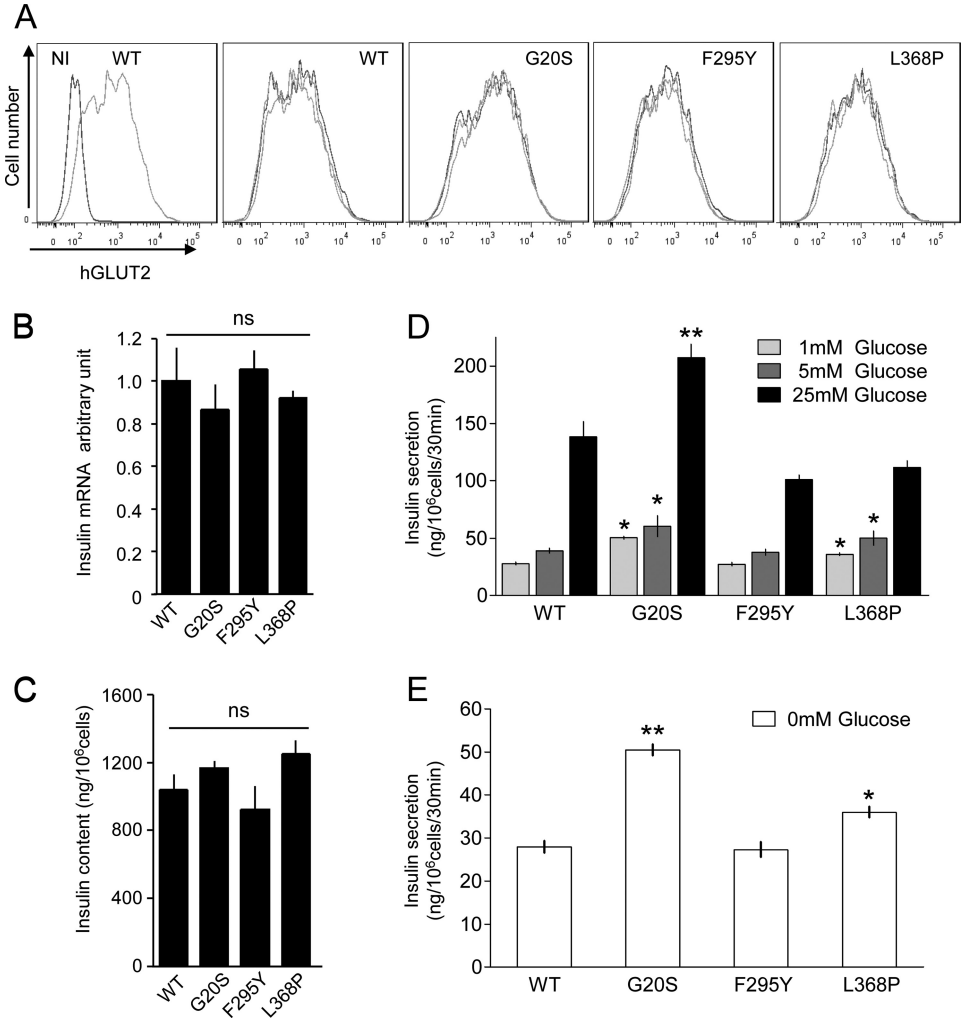

FIGURE 5. **Impact of G20S, F295Y and L368P hGLUT2 mutants on insulin secretion.** *A*, quantification by flow cytometry of plasma membrane expression for wild type (*WT*), G20S, F295Y, and L368P hGLUT2 in infected MIN6 cells that were cultured in 0 mM (*light gray*), 5 mM (*dark gray*), or 25 mM (*black*) glucose. Nonpermeabilized cells are labeled with an antibody to an extracellular epitope of hGLUT2. Noninfected cells (*NI*) are used as negative control. *B* and *C*, insulin mRNA levels (*B*) and protein contents (*C*) in MIN6 cells expressing WT, G20S, F295Y, or L368P hGLUT2 cultured in 25 mM glucose. *D*, glucose-induced insulin secretion by MIN6 cells expressing WT, G20S, F295Y, or L368P hGLUT2 in response to 1 mM (*light gray*), 5 mM (*dark gray*), or 25 mM (*black*) glucose. *E*, basal insulin secretion by MIN6 cells expressing WT, G20S, F295Y, or L368P hGLUT2 in the absence of glucose. *ns*, no significant differences between WT and mutants. *, $p < 0.05$; **, $p < 0.01$ comparison between WT and mutant hGLUT2 at the same glucose concentration.

positive cells (Fig. 6*E*) or amylase-positive cells (not shown) were not affected, suggesting that the increase in insulin-positive cell surface by the expression of mutated hGLUT2 could be attributed to differentiation and not to proliferation of β cells.

To assess the impact of mutants on the β cell function, glucose-induced insulin secretion per insulin-positive cell area was assayed in pancreatic explants infected with hGLUT2 mutants (Fig. 7*A*). We did not detect any significant difference between noninfected pancreases and pancreases infected with F295Y or L368P hGLUT2, suggesting that the F295Y hGLUT2 mutant modifies the number of β cells in the absence of glucose but not their capacity to secrete insulin in response to glucose as observed in MIN6 cells (Fig. 5*D*). On the contrary, expression of G20S hGLUT2 significantly increased glucose- induced insulin secretion per cell as shown in MIN6 cells (Fig. 5*D*). Electron microscopy analyses reveal that cell morphology is identical in noninfected and G20S hGLUT2-infected pancreases (Fig. 7, *B* and *C*). Dense core granules are shown in different pancreatic endocrine cell types. The immunogold labeling indicates that insulin-producing granules are characterized by a clear halo (Fig. 7*D*). The size of the insulin producing granules, assessed by diameter measurement of 600 granules, is significantly increased in G20S hGLUT2-infected pancreases (Fig. 7*E*). This is in good agreement with the immunofluorescence analyses and suggests that expression of this mutant accumulates insulin and enlarges granule size.

Finally, because the mutant F295Y increases the number of β cells in the absence of glucose and not the cell capacity to secrete insulin, we tested whether the increased number of β cells was dependent on the activation of ChREBP, a transcription factor mediating glucose-stimulated gene transcription (34) and described to regulate β cell number (33). In control noninfected pancreases, the positive effect of glucose on β cell number was prevented by infection with a dominant-negative form of ChREBP (not shown and Ref. 33). Co-expression of the dominant-negative form of ChREBP blocked the activating effect of F295Y hGLUT2 mutant on β cell number in the absence of glucose (Fig. 8*A*, with quantification in Fig. 8*B*). This

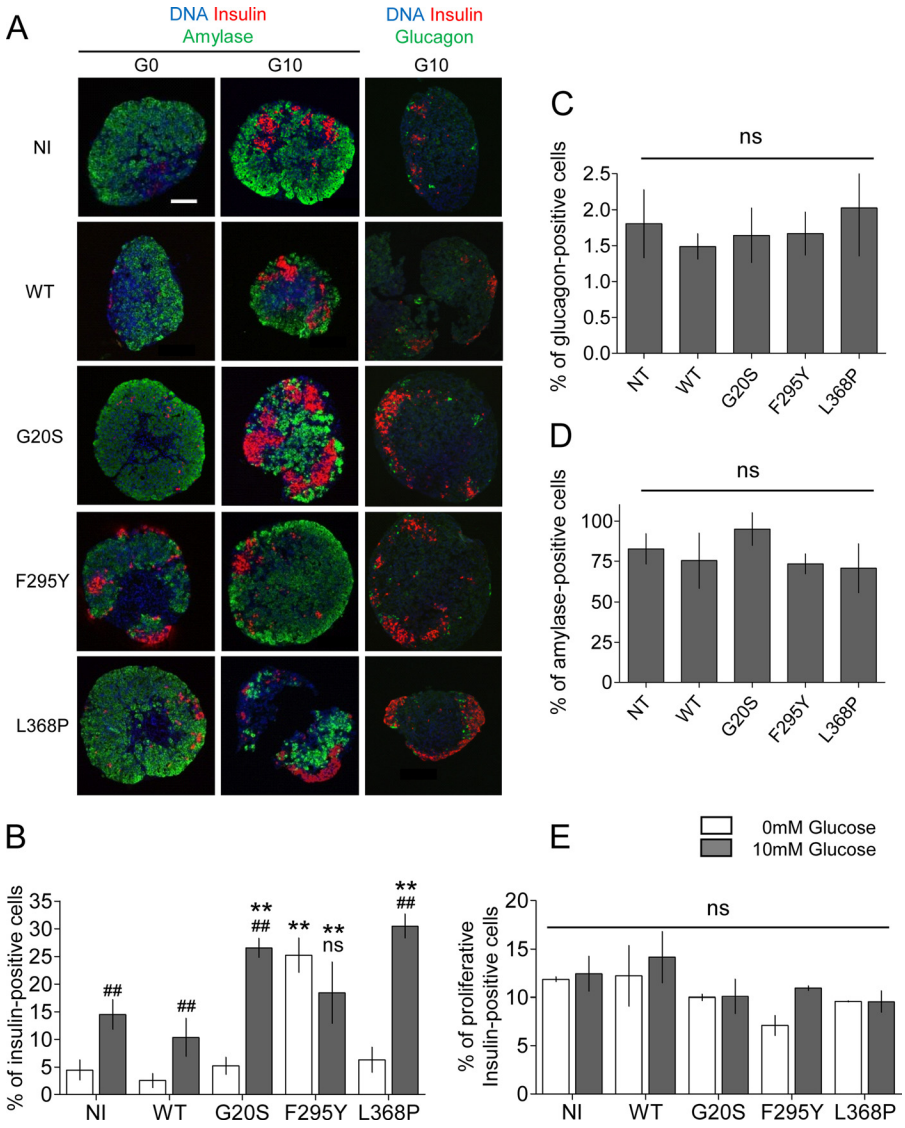

FIGURE 6. **G20S, F295Y, and L368P hGLUT2 mutants increase pancreatic β cell differentiation.** *A*, immunohistology analysis of rat pancreases cultured for 7 days in the absence (*left panels*) or presence (*middle* and *right panels*) of 10 mM glucose. Staining of insulin (*red*), amylase (*green*, *left* and *middle panels*), or glucagon (*green*, *right panels*) and nuclei (*blue*) in noninfected pancreas (*NI*), pancreas infected with an adenoviral vector encoding hGLUT2 wild type (*WT*), G20S, F295Y, or L368P. *Scale bar* corresponds to 100 μm. *B–D*, quantification of the surfaces occupied by insulin-positive (*B*), glucagon-positive (*C*), or amylase-positive (*D*) cells expressed as a percentage of total cell surface after 7 days of culture in 0 mM (*white bars*) or 10 mM glucose (*gray bars*) glucose. *E*, proliferative index of insulin-positive cells after 7 days of culture in 0 mM (*white bars*) or 10 mM (*gray bars*) glucose, as assayed by the frequency of BrdU-positive nuclei among insulin-positive cells. ##, $p < 0.01$. *ns*, nonsignificant, comparison between 10 and 0 mM glucose concentrations. **, $p < 0.01$ comparison between WT and mutant hGLUT2 at the same glucose concentration.

result suggests that ChREBP is a downstream actor of GLUT2 receptor signaling cascade involved in the regulation of β cell differentiation.

DISCUSSION

To characterize structure-function relationships of hGLUT2 for sugar transport and extracellular sugar detection and their impact on insulin secretion and β cell differentiation, we characterized mutations affecting various domains of hGLUT2. We took advantage of naturally occurring *SLC2A2* polymorphisms or FBS-associated mutations and completed the study with the design of mutations based on sequence alignment and conserved amino acids. None of the FBS-associated mutants could transport glucose to a significant level. This was either due to loss of protein expression at the plasma membrane (G20D and S242R) or to loss of transport capacity despite adequate membrane targeting (P417L and W444R), pointing out the crucial role of the last two amino acids (Pro-417 and Trp-444) for hGLUT2 transport function. In contrast, all the engineered mutants were correctly addressed at the plasma membrane but displayed altered transport kinetic parameters and increased insulin secretion and/or β cell differentiation. A salient discovery was that the three hGLUT2 mutants increased the insulin-positive cell number, highlighting the role of GLUT2 in pancreatic β cell development. This result is of most interest, knowing that, in rat, the expression of GLUT2 was detected as early as embryonic day 11.5, *i.e.*, before differentiation of pancreatic β cells (38). It is then tempting to propose that the early expression of this specific isoform of glucose transporter promotes pancreatic β cell development. Importantly, two hGLUT2

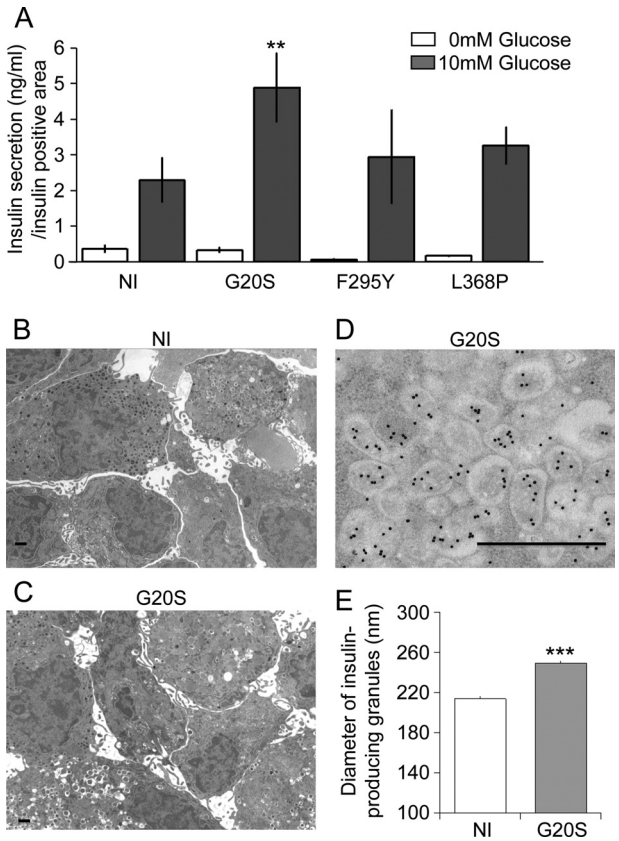

FIGURE 7. **Pancreatic β cells induced by G20S, F295Y, and L368P hGLUT2 mutants secrete insulin in response to glucose.** *A*, glucose-induced insulin secretion by rat pancreases noninfected (*NI*) or infected with an adenoviral vector encoding hGLUT2 G20S, F295Y, or L368P. **, $p < 0.01$ comparison between NI and mutant hGLUT2 at the same glucose concentration. *B* and *C*, morphological studies by electron microscopy of rat pancreases noninfected (*NI*) or infected with an adenoviral vector coding G20S hGLUT2 mutant after 7 days in culture. Type A cells (very dense core granules) and type B cells (dense core granules with halo) are both visible (×3,400). *Scale bar* corresponds to 1 μm. *D*, immunogold staining of insulin producing cells in a rat pancreas infected with an adenoviral vector coding G20S hGLUT2 mutant. Most of the secretory granules show labeling on the amorphous dense cores (×16,000). *Scale bar* corresponds to 1 μm. *E*, measurement of the diameter of 600 granules of insulin producing cells, using images at a magnification of 12,500. ***, $p < 0.001$ comparison with NI.

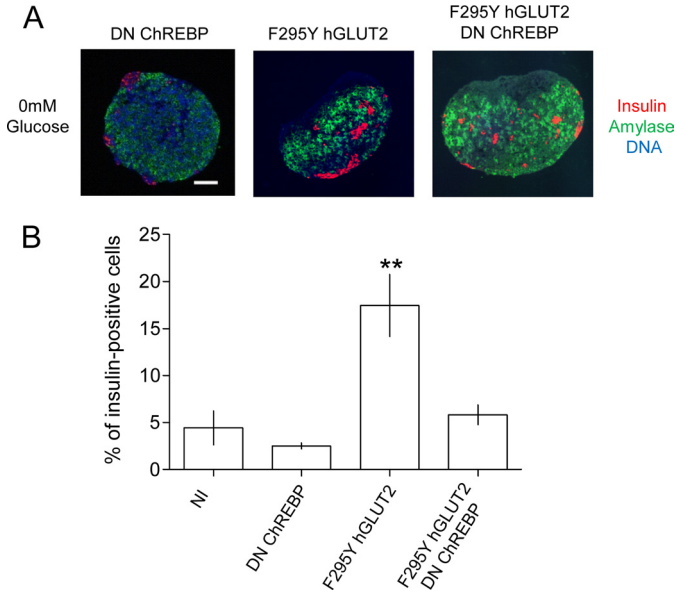

FIGURE 8. **F295Y hGLUT2 mutant increases pancreatic β cell differentiation through ChREBP activation.** *A*, immunohistology analysis of rat pancreases cultured for 7 days in the absence of glucose. Staining of insulin (*red*), amylase (*green*), and nuclei (*blue*) in pancreas infected with an adenoviral vector coding either a dominant-negative form of ChREBP (*DN ChREBP*), the F295Y hGLUT2 mutant, or both. *Scale bar* corresponds to 100 μm. *B*, quantification of the surfaces occupied by insulin-positive cells expressed as a percentage of total cell surface after 7 days of culture in 0 mM glucose. **, $p < 0.01$ comparison with NI.

mutants (G20S and L368P) increased basal insulin secretion in the absence of glucose disqualifying a role of metabolism alone in this process. Similarly, F295Y expression increased β cell development in the absence of glucose, suggesting that GLUT2 receptor function may be involved. Our data also suggest that the transcription factor ChREBP, known to regulate β cell development in response to glucose metabolism (33), may also be activated downstream activation of the receptor GLUT2 and in the absence of glucose metabolism. These are the first examples of gain of function mutations for the hGLUT2 protein affecting its receptor activity independently of its transporter activity.

This study improved our knowledge of GLUT2 structure-function map (Table 3). All the GLUT family members display 12 transmembrane domains (TMs). The N- and C-terminal domains, of six TMs each, are connected by a large intracellular loop (loop 6) (24). The two SNPs affect amino acids located in the first half of the protein (Pro-68 and Thr-110) and impaired neither the expression nor the transporter or receptor functions of hGLUT2. On the contrary, amino acid Gly-20 seems crucial, preventing expression when substituted to Asp and changing protein function and probably conformation when substituted to Ser. A family signature motif PESPR is located at the beginning of the sixth intracellular loop, Ser-242 substituted to an arginine lessened protein expression and location, blunting its transport activity. This is not in perfect accordance with the mutation of invariant S223A in XylE, which preserved 50% of transport activity (24), suggesting that another substitution for this amino acid (not affecting expression or membrane location) may reveal a partial effect on transport activity. Helices in TM 7 and TM 10 are discontinuous, allowing conformational changes during substrate transport (24). Leu-368, located at the beginning of TM 9, Pro-417 in TM 10, within the sugar tunnel, and Trp-444, a polar aromatic residue involved in the sugar-binding site, are highly conserved or invariant amino acids for the sugar porter family. They all reduced or blunted GLUT2 transport activity without affecting its expression. Finally, the amino acid Phe-295, located in intracellular loop 6, is highly conserved within the sugar porter family. This loop is mediating a GLUT2-specific sugar-signaling pathway involving interaction with import protein karyopherin α2 (4, 5, 7). When Phe-295 is mutated to an aromatic tyrosine residue, it may lock the receptor in an active conformation and perturb the signal transduction process by increasing activation of downstream effectors. The reverse impact of dominant-negative ChREBP on active F295Y hGLUT2 suggests that the signaling pathway downstream GLUT2 receptor may also involve ChREBP. In addition, the transcription factor ChREBP was shown to interact with karyopherin to translocate to the nucleus (39). It is thus tempting to propose the following GLUT2 receptor signaling pathway: karyopherin α that interacts directly with the cyto-

TABLE 3
Structure-function analysis of hGLUT2
Loop, loop between transmembrane domains; WT, wild-type hGLUT2; NA, nonapplicable; ND, not determined.

Mutation	Found in human	Amino acid location	Domain function	Plasma membrane expression	Transport activity	Receptor activity
G20D	FBS	TM1	Unknown	No	NA	ND
G20S		TM1	Unknown	Yes	High	High with or without glucose
P68L	SNP	Loop 1	Unknown	Yes	As WT	ND
T110I	SNP	TM2	Unknown	Yes	As WT	ND
S242R	FBS	Loop 6	PESPR signature	No	None	ND
F295Y		Loop 6	Signaling	Yes	Close to WT	High without glucose
L368P		TM9	Sugar tunnel	Yes	Low	High without glucose
P417L	FBS	TM10	Sugar tunnel	Yes	None	ND
W444R	FBS	TM11	Sugar-binding site	Yes	None	ND

plasmic loop of GLUT2 in the absence of extracellular sugar may be released in response to activation of the receptor by extracellular sugar, allowing nuclear translocation of ChREBP.

Several single-nucleotide polymorphisms have been described in human *SLC2A2*: some are located in the promoter (*e.g.*, rs5393 and rs5394), and others are located in the exons (rs5404 (T198T), rs5400 (T110I), and rs7637863 (P68L)). The association of some of these SNPs with type 2 diabetes is controversial (16–20). The SNP introducing a missense mutation in the protein, T110I, was first identified in 1994 in a genetic linkage analysis of acute insulin secretion in Pima Native Americans (40). Since then, this "historical" SNP of GLUT2 has been analyzed in numerous genetic studies, and conflicting conclusions were reached: the SNP T110I was found either associated (16, 17, 20) or not associated (19, 40) with a risk of type 2 diabetes. Other studies found this SNP to be associated with the conversion from impaired glucose tolerance to type 2 diabetes (18) or with hypercholesterolemia (41). During an oral glucose tolerance test performed on subjects stratified according to genotype of rs5400, no difference in insulin secretion was observed (17), suggesting that neither β cell mass nor insulin content are affected. Actually, this SNP is in strong linkage disequilibrium with two other polymorphisms located in the promoter region of the *SLC2A2* gene (18, 20). Thus, the functional consequence could be related to differences in GLUT2 protein levels but not to the effect of the variant hGLUT2 T110I *per se*. Interestingly, this hGLUT2 variant was associated with high daily consumption of sugars (42), suggesting a GLUT2-mediated glucose-sensing mechanism that could regulate food intake and sugar preference and thus subsequently be linked with risk of type 2 diabetes. Here we showed that the T110I variant displayed kinetic parameters for glucose transport similar to wild-type hGLUT2, in accordance with a previous report (28). This indicated that *SLC2A2* SNP links with sugar preference and type 2 diabetes were irrelevant to GLUT2 transport function. The second SNP characterized in this study, P68L, was detected in 1% of the population without any reported associated phenotype. The P68L hGLUT2 SNP transported less sugar per unit of transporter, but this feature did not seem to promote any homeostatic disturbance, at least in the physiological situation.

To date, the majority of *SLC2A2* gene mutations related to FBS have been investigated by DNA screening. In this work, we fully characterized four FBS-associated *SLC2A2* missense mutations. The resulting hGLUT2 mutants displayed a total loss of transport function despite protein biosynthesis and plasma membrane targeting similar to wild-type protein for two of them. The syndrome of the patients carrying these mutations can therefore be attributed to the lack of GLUT2 transport activity. Recently, compound heterozygous *SLC2A2* mutations characterized by a deletion p.153–4delLI associated with a missense mutation P417R has been linked with mild Fanconi-Bickel syndrome (mild glucosuria) (43). Here, we showed that leucine substitution (P417L) abolished transport activity. One can anticipate that arginine substitution (P417R) may conserve a weak GLUT2 transport activity as compared with P417L mutant explaining the mild phenotype. It would be interesting to document the minimal reduction in hGLUT2 activity required to induce development of phenotypic traits of FBS, according to tissue damages. Indeed, in GLUT1 deficiency syndrome, only mutations retaining more than 50% of transport activity are compatible with human life by fulfilling the sugar needs of the brain (44). The variable penetrance of the hGLUT2 deficiency (*i.e.*, FBS) might be reflecting the glucose needs of each tissue.

The engineered mutations in *SLC2A2* modified glucose transport parameters, but functional consequences were difficult to predict. Nevertheless, profound modulations in insulin-producing pancreatic β cell differentiation and function occurred. Increased insulin secretion or pancreatic β cell differentiation in response to glucose induced by expression of G20S mutant may be explained by its increased V_{max}. However, increased glucose-independent basal insulin secretion by expression of G20S and L368P mutants indicated a constitutive activation of hGLUT2 receptor function independent of its transporter kinetic parameters. The sugar signaling pathway triggered by GLUT2 is known to control expression of glucose-sensitive genes (3, 6, 32) that might boost insulin secretion in MIN6 cells (45) or insulin accumulation in granules (46) as we observed in pancreases. Conformational changes induced by these mutations might lead to a better intrinsic signaling capacity of GLUT2 (8). Furthermore, F295Y mutant induced pancreatic β cell development in glucose-deprived culture, to the level of differentiation reached in high glucose concentrations. This also suggests a constitutively activated conformation of the F295Y-mutated protein.

We described here four loss of function and three gain of function mutations in *SLC2A2* coding the human GLUT2 transporter. The loss of function mutations were responsible for the Fanconi-Bickel syndrome. Gain of function hGLUT2 mutations could accelerate β cell differentiation, and a higher β cell number would secrete more insulin. In addition, a β cell equipped with activating hGLUT2 mutants, showing a better affinity for sugar, higher maximal transport rate, or constitu-

tively activated receptor, would further increase insulin secretion per cell unit. The role of GLUT2 is thus important during embryonic period for differentiation of insulin-producing cells and insulin secretion. We imagine that activating mutation in *SLC2A2* could be responsible *in vivo* for syndrome with increased insulin secretion as observed in congenital hyperinsulinism (47). Knowing that for 40–50% of all congenital hyperinsulinism cases, it is necessary to uncover other mutated genes than the genes coding the two subunits of the ATP-dependent potassium channel, we propose *SLC2A2* to be sequenced in congenital hyperinsulinism patients sensitive to K^+ATP channel opener treatment (diazoxide) and for which no mutations in identified genes were found.

In conclusion, through the study of a panel of mutations in *SLC2A2*, we deciphered how two complementary functions of hGLUT2, sugar transporter and extracellular sugar receptor, impact on insulin secretion and pancreatic β cell differentiation. Because gain of function mutations of hGLUT2 activated β cell development or insulin secretion but only mildly affected transport, it could be of interest to develop pharmacological tools for metabolic diseases, targeting the receptor function of hGLUT2 without affecting vital sugar provision by hGLUT2 transporter.

Acknowledgments—We thank Abdelhamid Benkouhi, Anne Houllier, and Kathleen Flosseau for technical assistance. M. L. G. thanks Lionel Arnaud for discussion and support all through this project.

REFERENCES

1. Thorens, B., Charron, M. J., and Lodish, H. F. (1990) Molecular physiology of glucose transporters. *Diabetes Care* **13,** 209–218
2. Matschinsky, F. M. (1990) Glucokinase as glucose sensor and metabolic signal generator in pancreatic β-cells and hepatocytes. *Diabetes* **39,** 647–652
3. Guillemain, G., Loizeau, M., Pinçon-Raymond, M., Girard, J., and Leturque, A. (2000) The large intracytoplasmic loop of the glucose transporter GLUT2 is involved in glucose signaling in hepatic cells. *J. Cell Sci.* **113,** 841–847
4. Guillemain, G., Muñoz-Alonso, M. J., Cassany, A., Loizeau, M., Faussat, A. M., Burnol, A. F., and Leturque, A. (2002) Karyopherin α2. A control step of glucose-sensitive gene expression in hepatic cells. *Biochem. J.* **364,** 201–209
5. Cassany, A., Guillemain, G., Klein, C., Dalet, V., Brot-Laroche, E., and Leturque, A. (2004) A karyopherin α2 nuclear transport pathway is regulated by glucose in hepatic and pancreatic cells. *Traffic* **5,** 10–19
6. Le Gall, M., Tobin, V., Stolarczyk, E., Dalet, V., Leturque, A., and Brot-Laroche, E. (2007) Sugar sensing by enterocytes combines polarity, membrane bound detectors and sugar metabolism. *J. Cell Physiol.* **213,** 834–843
7. Guillemain, G., Da Silva Xavier, G., Rafiq, I., Leturque, A., and Rutter, G. A. (2004) Importin β1 mediates the glucose-stimulated nuclear import of pancreatic and duodenal homeobox-1 in pancreatic islet β-cells (MIN6). *Biochem. J.* **378,** 219–227
8. Leturque, A., Brot-Laroche, E., and Le Gall, M. (2009) GLUT2 mutations, translocation, and receptor function in diet sugar managing. *Am. J. Physiol. Endocrinol. Metab.* **296,** E985–E992
9. Levy, S., Kafri, M., Carmi, M., and Barkai, N. (2011) The competitive advantage of a dual-transporter system. *Science* **334,** 1408–1412
10. Santer, R., Steinmann, B., and Schaub, J. (2002) Fanconi-Bickel syndrome. A congenital defect of facilitative glucose transport. *Curr. Mol. Med.* **2,** 213–227
11. Pena, L., and Charrow, J. (2011) Fanconi-Bickel syndrome. Report of life history and successful pregnancy in an affected patient. *Am. J. Med. Genet. A* **155A,** 415–417
12. Taha, D., Al-Harbi, N., and Al-Sabban, E. (2008) Hyperglycemia and hypoinsulinemia in patients with Fanconi-Bickel syndrome. *J. Pediatr. Endocrinol. Metab.* **21,** 581–586
13. Ganesh, R., Arvindkumar, R., and Vasanthi, T. (2009) Infantile-onset diabetes mellitus. A 1-year follow-up study. *Clin. Pediatr.* (*Phila.*) **48,** 271–274
14. Sansbury, F. H., Flanagan, S. E., Houghton, J. A., Shuixian Shen, F. L., Al-Senani, A. M., Habeb, A. M., Abdullah, M., Kariminejad, A., Ellard, S., and Hattersley, A. T. (2012) SLC2A2 mutations can cause neonatal diabetes, suggesting GLUT2 may have a role in human insulin secretion. *Diabetologia* **55,** 2381–2385
15. Hughes, S. D., Quaade, C., Johnson, J. H., Ferber, S., and Newgard, C. B. (1993) Transfection of AtT-20ins cells with GLUT-2 but not GLUT-1 confers glucose-stimulated insulin secretion. Relationship to glucose metabolism. *J. Biol. Chem.* **268,** 15205–15212
16. Barroso, I., Luan, J., Middelberg, R. P., Harding, A. H., Franks, P. W., Jakes, R. W., Clayton, D., Schafer, A. J., O'Rahilly, S., and Wareham, N. J. (2003) Candidate gene association study in type 2 diabetes indicates a role for genes involved in β-cell function as well as insulin action. *PLoS Biol.* **1,** E20
17. Burgdorf, K. S., Grarup, N., Justesen, J. M., Harder, M. N., Witte, D. R., Jørgensen, T., Sandbaek, A., Lauritzen, T., Madsbad, S., Hansen, T., and Pedersen, O. (2011) Studies of the association of Arg72Pro of tumor suppressor protein p53 with type 2 diabetes in a combined analysis of 55,521 Europeans. *PLoS One* **6,** e15813
18. Laukkanen, O., Lindström, J., Eriksson, J., Valle, T. T., Hämäläinen, H., Ilanne-Parikka, P., Keinänen-Kiukaanniemi, S., Tuomilehto, J., Uusitupa, M., and Laakso, M. (2005) Polymorphisms in the SLC2A2 (GLUT2) gene are associated with the conversion from impaired glucose tolerance to type 2 diabetes. The Finnish Diabetes Prevention Study. *Diabetes* **54,** 2256–2260
19. Møller, A. M., Jensen, N. M., Pildal, J., Drivsholm, T., Borch-Johnsen, K., Urhammer, S. A., Hansen, T., and Pedersen, O. (2001) Studies of genetic variability of the glucose transporter 2 promoter in patients with type 2 diabetes mellitus. *J. Clin. Endocrinol. Metab.* **86,** 2181–2186
20. Willer, C. J., Bonnycastle, L. L., Conneely, K. N., Duren, W. L., Jackson, A. U., Scott, L. J., Narisu, N., Chines, P. S., Skol, A., Stringham, H. M., Petrie, J., Erdos, M. R., Swift, A. J., Enloe, S. T., Sprau, A. G., Smith, E., Tong, M., Doheny, K. F., Pugh, E. W., Watanabe, R. M., Buchanan, T. A., Valle, T. T., Bergman, R. N., Tuomilehto, J., Mohlke, K. L., Collins, F. S., and Boehnke, M. (2007) Screening of 134 single nucleotide polymorphisms (SNPs) previously associated with type 2 diabetes replicates association with 12 SNPs in nine genes. *Diabetes* **56,** 256–264
21. Richardson, C. C., Hussain, K., Jones, P. M., Persaud, S., Löbner, K., Boehm, A., Clark, A., and Christie, M. R. (2007) Low levels of glucose transporters and K^+ATP channels in human pancreatic β cells early in development. *Diabetologia* **50,** 1000–1005
22. Abramson, J., Smirnova, I., Kasho, V., Verner, G., Kaback, H. R., and Iwata, S. (2003) Structure and mechanism of the lactose permease of Escherichia coli. *Science* **301,** 610–615
23. Dang, S., Sun, L., Huang, Y., Lu, F., Liu, Y., Gong, H., Wang, J., and Yan, N. (2010) Structure of a fucose transporter in an outward-open conformation. *Nature* **467,** 734–738
24. Sun, L., Zeng, X., Yan, C., Sun, X., Gong, X., Rao, Y., and Yan, N. (2012) Crystal structure of a bacterial homologue of glucose transporters GLUT1–4. *Nature* **490,** 361–366
25. Carruthers, A., DeZutter, J., Ganguly, A., and Devaskar, S. U. (2009) Will the original glucose transporter isoform please stand up! *Am. J. Physiol. Endocrinol. Metab.* **297,** E836–E848
26. Salas-Burgos, A., Iserovich, P., Zuniga, F., Vera, J. C., and Fischbarg, J. (2004) Predicting the three-dimensional structure of the human facilitative glucose transporter glut1 by a novel evolutionary homology strategy. Insights on the molecular mechanism of substrate migration, and binding sites for glucose and inhibitory molecules. *Biophys. J.* **87,** 2990–2999
27. Hruz, P. W., and Mueckler, M. M. (2001) Structural analysis of the GLUT1 facilitative glucose transporter (review). *Mol. Membr. Biol.* **18,** 183–193
28. Mueckler, M., Kruse, M., Strube, M., Riggs, A. C., Chiu, K. C., and Permutt,

M. A. (1994) A mutation in the Glut2 glucose transporter gene of a diabetic patient abolishes transport activity. *J. Biol. Chem.* **269,** 17765–17767
29. Grand, T., L'Hoste, S., Mordasini, D., Defontaine, N., Keck, M., Pennaforte, T., Genete, M., Laghmani, K., Teulon, J., and Lourdel, S. (2011) Heterogeneity in the processing of CLCN5 mutants related to Dent disease. *Hum. Mutat.* **32,** 476–483
30. Antoine, B., Levrat, F., Vallet, V., Berbar, T., Cartier, N., Dubois, N., Briand, P., and Kahn, A. (1992) Gene expression in hepatocyte-like lines established by targeted carcinogenesis in transgenic mice. *Exp. Cell Res.* **200,** 175–185
31. Miyazaki, J., Araki, K., Yamato, E., Ikegami, H., Asano, T., Shibasaki, Y., Oka, Y., and Yamamura, K. (1990) Establishment of a pancreatic β cell line that retains glucose-inducible insulin secretion. Special reference to expression of glucose transporter isoforms. *Endocrinology* **127,** 126–132
32. Stolarczyk, E., Le Gall, M., Even, P., Houllier, A., Serradas, P., Brot-Laroche, E., and Leturque, A. (2007) Loss of sugar detection by GLUT2 affects glucose homeostasis in mice. *PLoS One* **2,** e1288
33. Soggia, A., Flosseau, K., Ravassard, P., Szinnai, G., Scharfmann, R., and Guillemain, G. (2012) Activation of the transcription factor carbohydrate-responsive element-binding protein by glucose leads to increased pancreatic β cell differentiation in rats. *Diabetologia* **55,** 2713–2722
34. Tsatsos, N. G., Davies, M. N., O'Callaghan, B. L., and Towle, H. C. (2008) Identification and function of phosphorylation in the glucose-regulated transcription factor ChREBP. *Biochem. J.* **411,** 261–270
35. Gould, G. W., Thomas, H. M., Jess, T. J., and Bell, G. I. (1991) Expression of human glucose transporters in *Xenopus* oocytes. Kinetic characterization and substrate specificities of the erythrocyte, liver, and brain isoforms. *Biochemistry* **30,** 5139–5145
36. Clark, S. A., Quaade, C., Constandy, H., Hansen, P., Halban, P., Ferber, S., Newgard, C. B., and Normington, K. (1997) Novel insulinoma cell lines produced by iterative engineering of GLUT2, glucokinase, and human insulin expression. *Diabetes* **46,** 958–967
37. Guillemain, G., Filhoulaud, G., Da Silva-Xavier, G., Rutter, G. A., and Scharfmann, R. (2007) Glucose is necessary for embryonic pancreatic endocrine cell differentiation. *J. Biol. Chem.* **282,** 15228–15237
38. Pang, K., Mukonoweshuro, C., and Wong, G. G. (1994) β cells arise from glucose transporter type 2 (Glut2)-expressing epithelial cells of the developing rat pancreas. *Proc. Natl. Acad. Sci. U.S.A.* **91,** 9559–9563
39. Ge, Q., Nakagawa, T., Wynn, R. M., Chook, Y. M., Miller, B. C., and Uyeda, K. (2011) Importin-α protein binding to a nuclear localization signal of carbohydrate response element-binding protein (ChREBP). *J. Biol. Chem.* **286,** 28119–28127
40. Janssen, R. C., Bogardus, C., Takeda, J., Knowler, W. C., and Thompson, D. B. (1994) Linkage analysis of acute insulin secretion with GLUT2 and glucokinase in Pima Indians and the identification of a missense mutation in GLUT2. *Diabetes* **43,** 558–563
41. Igl, W., Johansson, A., Wilson, J. F., Wild, S. H., Polasek, O., Hayward, C., Vitart, V., Hastie, N., Rudan, P., Gnewuch, C., Schmitz, G., Meitinger, T., Pramstaller, P. P., Hicks, A. A., Oostra, B. A., van Duijn, C. M., Rudan, I., Wright, A., Campbell, H., and Gyllensten, U. (2010) Modeling of environmental effects in genome-wide association studies identifies SLC2A2 and HP as novel loci influencing serum cholesterol levels. *PLoS Genet.* **6,** e1000798
42. Eny, K. M., Wolever, T. M., Fontaine-Bisson, B., and El-Sohemy, A. (2008) Genetic variant in the glucose transporter type 2 is associated with higher intakes of sugars in two distinct populations. *Physiol. Genomics* **33,** 355–360
43. Grünert, S. C., Schwab, K. O., Pohl, M., Sass, J. O., and Santer, R. (2012) Fanconi-Bickel syndrome. GLUT2 mutations associated with a mild phenotype. *Mol. Genet. Metab.* **105,** 433–437
44. Yang, H., Wang, D., Engelstad, K., Bagay, L., Wei, Y., Rotstein, M., Aggarwal, V., Levy, B., Ma, L., Chung, W. K., and De Vivo, D. C. (2011) Glut1 deficiency syndrome and erythrocyte glucose uptake assay. *Ann. Neurol.* **70,** 996–1005
45. Schuit, F., Flamez, D., De Vos, A., and Pipeleers, D. (2002) Glucose-regulated gene expression maintaining the glucose-responsive state of β-cells. *Diabetes* **51,** S326–S332
46. Hou, J. C., Min, L., and Pessin, J. E. (2009) Insulin granule biogenesis, trafficking and exocytosis. *Vitam. Horm.* **80,** 473–506
47. Giurgea, I., Bellanné-Chantelot, C., Ribeiro, M., Hubert, L., Sempoux, C., Robert, J. J., Blankenstein, O., Hussain, K., Brunelle, F., Nihoul-Fékété, C., Rahier, J., Jaubert, F., and de Lonlay, P. (2006) Molecular mechanisms of neonatal hyperinsulinism. *Horm. Res.* **66,** 289–296